Applied Mathematics and Computation 324 (2018) 141–155

Contents lists available at ScienceDirect

Applied Mathematics and Computation

journal homepage: www.elsevier.com/locate/amc

A modified SEIR model for the spread of Ebola in Western Africa and metrics for resource allocation☆

Paul Diaz[a], Paul Constantine[b], Kelsey Kalmbach[c], Eric Jones[d], Stephen Pankavich[c,*]

[a] Department of Aerospace Engineering Sciences, University of Colorado, Boulder, CO 80309, United States
[b] Department of Computer Science, University of Colorado, Boulder, CO 80309, United States
[c] Department of Applied Mathematics and Statistics, Colorado School of Mines, 1500 Illinois St., Golden, CO 80401, United States
[d] Department of Physics, University of California at Santa Barbara, Santa Barbara, CA 93106, United States

ARTICLE INFO

MSC:
92D30
37N25
34D20
92B05
92D25

Keywords:
Epidemiology
Ebola
Uncertainty quantification
Active subspaces
Stability

ABSTRACT

A modified, deterministic SEIR model is developed for the 2014 Ebola epidemic occurring in the West African nations of Guinea, Liberia, and Sierra Leone. The model describes the dynamical interaction of susceptible and infected populations, while accounting for the effects of hospitalization and the spread of disease through interactions with deceased, but infectious, individuals. Using data from the World Health Organization (WHO), parameters within the model are fit to recent estimates of infected and deceased cases from each nation. The model is then analyzed using these parameter values. Finally, several metrics are proposed to determine which of these nations is in greatest need of additional resources to combat the spread of infection. These include local and global sensitivity metrics of both the infected population and the basic reproduction number with respect to rates of hospitalization and proper burial.

1. Introduction

The most recent Ebola outbreak began in December 2013 and resulted in a devastating loss of life in Guinea, Liberia, and Sierra Leone. This outbreak has been the deadliest in the history of the disease claiming more than 10,000 lives to date [4,22]. The severity of the epidemic has prompted an international response to halt further spread of the disease. In particular, efforts arising within the United States and China have provided additional relief to the region, but within 2014 this had not been enough to end the epidemic.

Some basic facts about Ebola disease pathogenesis are well known. Those exposed to the virus experience an 8-to-10 day average incubation period during which they remain noninfectious [4], though the time between exposure and the onset of symptoms ranges from 2 to 21 days [9]. Once a patient becomes symptomatic, the virus may be transferred to others through direct contact with bodily fluids [10], such as blood and vomit. One important epidemiological feature of Ebola is that those who are killed by the disease can still transmit the virus to susceptible individuals. Unlike most pathogens, which

☆ The authors were supported by the joint Mathematical Association of America (MAA) and Society for Industrial and Applied Mathematics (SIAM) PIC Math program funded by the National Science Foundation (NSF grant no. DMS-1345499). Additionally, Stephen Pankavich was supported by the National Science Foundation under award DMS-1211667.

* Corresponding author.
E-mail address: pankavic@mines.edu (S. Pankavich).

https://doi.org/10.1016/j.amc.2017.11.039
0096-3003/

cannot survive long on a deceased individual, Ebola does remain infectious after a person succumbs to the disease [9]. In fact, the deceased are even more contagious than living Ebola patients as the virus can force a victim's body to release infectious fluids including blood, vomit, and fecal matter - especially in later stages of the disease [5]. This fluid release is among the most visually harrowing symptoms of Ebola, present in some late-stage patients [9].

The spread of infection from deceased to susceptible individuals is a significant problem in Western Africa where local burial rituals often require washing, touching, or kissing the body of the deceased. Among the traditional practices the WHO cautions against with Ebola victims are family-led body preparation and religious rituals that require direct contact with the corpse. Muslim tradition, for instance, requires that family members of the same gender wash the body themselves before burial. Moreover, the lack of adequate health care within Guinea, Liberia, and Sierra Leone has perpetuated the disease, as improper and unsafe burials place further individuals at risk. Widespread reports from Liberia in late 2014 described Ebola victims laying on the streets for days, drastically increasing the risk of infection [20]. The WHO estimates that contact with deceased individuals has caused at least 20% of all infections [21]. Hence, the bodies of deceased Ebola victims that have not been properly disposed and burial ceremonies, in which mourners have direct contact with the body of the deceased, can play a large role in the transmission of the virus, and these effects cannot be neglected within an informative model.

Another important feature is the effect of hospitalization. Due to their frequent interaction with patients either under investigation or confirmed to have contracted the Ebola virus, healthcare personnel are particularly susceptible to the disease [23]. In particular, they can be exposed to Ebola by coming in contact with a patient's body fluids, contaminated medical supplies and equipment, or contaminated environmental surfaces. For these reasons transmission between infectious, hospitalized individuals and medical workers are non-negligible within a descriptive epidemic model. Additionally, hospitalization and subsequent treatment does improve an infected patient's chances of recovery, though the difference in case fatality rates between hospitalized patients and non-hospitalized cases is relatively small [19], and an increase in the use of medical facilities within a population can reduce the damage caused by the epidemic.

While a previous study focused predominantly on the effects of contact tracing [18], it has recently been determined [13,15] that multiple aspects of disease pathogenesis, including hospitalization, case isolation, and further introduction of sanitary funeral processes, must be better addressed in order to fully mitigate further spread of the disease. Hence, the ultimate goal of the current study is to construct a model for the most recent Ebola epidemic in Western African and identify useful metrics to determine which of the affected countries would benefit most from the allocation of additional resources, including new treatment facilities or greater manpower to ensure proper burials. To this end, a deterministic model for the epidemic is constructed in the next section by accounting for the specific characteristics of the disease, including the incubation period, increased risk of infection from deceased individuals, and the effects of hospitalization. Realistic parameter values are determined by fitting to given data for each of the nations and a separate analysis of the respective reproduction numbers is conducted. In Section 3, we discuss local metrics other than direct computation of the basic reproduction number (R_0) which may allow one to determine the optimal sites for resource allocation and inhibit the spread of the disease. These metrics include fitted parameter values, the local sensitivity of the infectious population, and the local minimization of R_0 with respect to parameter variation. Within Section 4, we propose and explore a new method to compute the global sensitivity of R_0 with respect to alterations in the most crucial parameter values. Ultimately, we find that of these three troubled nations, it is Liberia that would benefit most from the introduction of additional medical resources. In general, these tools – especially the proposed activity scores of Section 4 – can be used to analyze future outbreaks in addition to the most recent crisis. Finally, the relevant details of computations are contained within the Appendix.

2. A mathematical model for Ebola

Our first objective is to develop a mathematical model for the spread of Ebola in Western Africa by accounting for the specific characteristics of the disease. SEIR models are often implemented when studying the spread of infectious diseases that possess significant incubation periods [1,11,15,16,18]. To describe the spread of Ebola, a traditional SEIR model is augmented with additional compartments based on the following assumptions. First, as the number of susceptibles is large, we neglect stochastic effects and formulate a deterministic model. Additionally, though the current epidemic has lasted for over a year, we assume that the outbreak is not sustained by the introduction of new susceptible individuals. Hence, national populations are near equilibrium and both births and deaths are neglected amongst the total population. We further assume that infected individuals can move to three different removed compartments: removed and infectious (i.e. not properly buried), removed and properly buried, and removed and recovered. This distinction is introduced to allow for the scenario in which individuals who have died from the disease, but have not been properly buried, may continue to infect susceptible individuals whom they contact.

We assume that those who recover from the disease are no longer susceptible, as survivors of Ebola are thought to be immune to the strain of the virus that infected them [5]. Once hospitalized, infected individuals can still spread the disease to members of the susceptible population. However, we assume that patients who die within a hospital receive an immediate proper burial, and thus cannot infect others once deceased. Finally, we assume that hospitalized individuals have a greater chance of survival than infected, non-hospitalized individuals [9]. This is consistent with estimates of the general Ebola fatality rate around 70% and the hospitalized fatality rate near 64% [19].

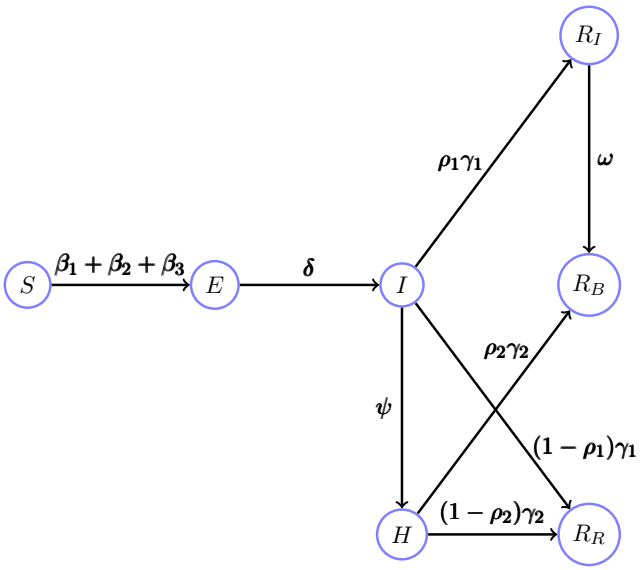

Fig. 1. A graph representing the states (S, E, I, R_B, R_I, R_R, and H) and transition pathways (arrows) in the Ebola model (1). Table 1 further describes the model parameters included above.

Table 1
Parameters in the Ebola dynamics model.

Parameter	Description
β_1	Transmission rate between infected and susceptible
β_2	Transmission rate between removed but still infectious and susceptible
β_3	Transmission rate between hospitalized and susceptible
δ	(Incubation period)$^{-1}$
γ_1	(Average time with disease for unhospitalized individuals)$^{-1}$
γ_2	(Average time with disease for hospitalized individuals)$^{-1}$
ψ	(Average time for infected to become hospitalized)$^{-1}$
ρ_1	Proportion of infected who die of the disease and are not hospitalized
ρ_2	Proportion of infected who die of the disease and are hospitalized
ω	(Average time until a deceased individual is properly buried)$^{-1}$

2.1. A modified SEIR model

With the aforementioned assumptions identified, we formulate a modified SEIR model to account for the dynamics of the disease within a population. The model consists of the following seven states, each a function of time t: (i) the susceptible proportion of the population $S(t)$, (ii) the exposed proportion (i.e., infected but asymptomatic) $E(t)$, (iii) the infectious and symptomatic proportion $I(t)$, (iv) the infectious and hospitalized proportion $H(t)$, (v) the removed but infectious proportion (i.e., those who died from the disease but have not been sanitarily buried) $R_I(t)$, (vi) the removed and buried proportion $R_B(t)$, and (vii) the removed and recovered proportion $R_R(t)$.

There are several ways in which the populations may be altered. First, susceptibles transfer to the exposed population after coming into contact with either an infectious individual (including those who are hospitalized) or a body which is not yet buried. After the viral incubation period, all exposed individuals move to the infectious population. The infectious move to one of three populations: hospitalized, removed and infectious, or removed and recovered. Note that infectious individuals cannot move immediately to a removed and buried state since we assume that some time is needed to bury an individual not receiving medical care at death. However, a proportion of removed and infectious individuals transfer to removed and buried. Hospitalized individuals move to either removed and buried or removed and recovered. Finally, all transmission terms are assumed to be of standard incidence form. Fig. 1 summarizes these transition pathways between populations, while Table 1 summarizes model parameters—all of which are nonnegative.

The coupled system of differential equations for $S(t)$, $E(t)$, $I(t)$, $H(t)$, and $R_I(t)$ is given by

$$\left.\begin{aligned}\frac{dS}{dt} &= -\beta_1 SI - \beta_2 SR_I - \beta_3 SH\\ \frac{dE}{dt} &= \beta_1 SI + \beta_2 SR_I + \beta_3 SH - \delta E\\ \frac{dI}{dt} &= \delta E - \gamma_1 I - \psi I\\ \frac{dH}{dt} &= \psi I - \gamma_2 H\\ \frac{dR_I}{dt} &= \rho_1\gamma_1 I - \omega R_I.\end{aligned}\right\} \tag{1}$$

The R_B and R_R proportions decouple from the system above as their values are determined once the others are known. Their respective time evolution is given by

$$\left.\begin{aligned}\frac{dR_B}{dt} &= \omega R_I + \rho_2\gamma_2 H\\ \frac{dR_R}{dt} &= (1-\rho_1)\gamma_1 I + (1-\rho_2)\gamma_2 H.\end{aligned}\right\} \tag{2}$$

With R_B and R_R accounted for, the model is conservative, and compartments here have been rescaled so that each uppercase variable represents the proportion of a specific population with respect to the total population. For example, letting lowercase variables ($s(t)$, $e(t)$, ...) denote total population counts within each compartment and denoting the total population constant by $N = s + e + i + h + r_i + r_b + r_r$, we see that $\frac{dN}{dt} = 0$. Hence, we can express the proportion of susceptible individuals as $S(t) = \frac{s(t)}{N}$ with analogous representations for the other dependent variables, and the model (1)–(2) follows. We note that this model is similar to a stochastic SEIR model derived in [11] to explain previous outbreaks in Uganda, Gabon, Sudan, and the Democratic Republic of the Congo. However, we employ a deterministic model herein and specifically assume that, due to current public health intervention, any individuals who die while hospitalized are properly buried. Additionally, the removed population within our model is separated into deceased (and noninfectious) and recovered individuals in order to provide more reasonable estimates of the impact of the disease.

2.2. Parameter fitting

We begin our analysis of the model by identifying values of model parameters that generate predictions matching available data for Guinea, Liberia, and Sierra Leone. We obtained time-series data for each nation from WHO Situation reports [22] and the Network Dynamics and Simulation Science Laboratory at Virginia Tech [14]. The data sets contain cumulative values of infections and deaths from each nation. However, the data are incomplete and/or irregularly reported; hence, we remove outliers and time periods without sufficient reporting. The remaining number of data points are 36, 90, and 61 for Liberia, Guinea, and Sierra Leone, respectively.

Since the data represent cumulative quantities, but the model describes instantaneous proportions of active infections, and differing compartments are employed in our model for deaths, a direct fit is not immediately possible. Instead, to generate cumulative quantities, the time-integrated infected population was fit to the cumulative infected data. Also, our model includes three deceased states, while the data do not differentiate among differing death compartments. Thus, we assume reported deaths in the data correspond to the properly buried population R_B, and not the deceased but infectious population R_I, as the latter are likely unknown to data collectors.

To fit the model parameters, an unconstrained nonlinear optimization was performed using MATLAB's `fminsearch` function, which utilizes a Nelder–Mead direct search method. Within this solver nonlinear parameter constraints were enforced by using a barrier function to ensure positive, realistic parameter values. The objective function, $D(\mathbf{p})$, where $\mathbf{p}$ represents the vector of parameters listed in Table 1, is defined as

$$D(\mathbf{p}) \;:=\; \sum_{t\in\mathcal{T}} [R_{data}(t) - N\cdot R_B(t;\mathbf{p})]^2 + \left[C_{data}(t) - N\cdot\delta\int_0^t E(s;\mathbf{p})\,ds\right]^2 \tag{3}$$

where $\mathcal{T}$ is the discrete set of times at which the data is available, N is the total population for a given nation, $R_{data}(t)$ is the recorded number of cumulative deceased individuals, and $C_{data}(t)$ is the recorded number of cumulative infections. The initial conditions are the proportions as of March 22, 2014. For example, the total estimated population of Liberia is $N = 4.29$ million, while the number of reported infections on this date was 9, and hence $I(0) = 9/(4.29\times 10^6) = 2.1\times 10^{-6}$.

Table 2 displays the fitted parameter values for each independent country. Estimates of the incubation period range between 8 and 10 days, so the daily probability of transition from the exposed state to the infected state was assumed to be $\delta = \frac{1}{9}$ for simplicity. Fig. 2 displays model trajectories with fitted parameters compared to the available data for Guinea, Liberia, and Sierra Leone.

Table 2
Fitted parameter values for each country. All parameters have the units of (days)$^{-1}$, with the exception of ρ_1 and ρ_2, which are dimensionless. The parameter δ was not fit, but taken directly from [9], while initial guesses for ρ_1 and ρ_2 were motivated by Dixon et al. [9].

Parameter	Guinea	Liberia	Sierra Leone	Source
β_1	0.315	0.376	0.251	Fit
β_2	0.16	0.135	0.395	Fit
β_3	0.0165	0.163	0.079	Fit
δ	$\frac{1}{9}$	$\frac{1}{9}$	$\frac{1}{9}$	[9]
γ_1	0.295	0.0542	0.051	Fit
γ_2	0.016	0.174	0.0833	Fit
ψ	0.500	0.500	0.442	Fit
ρ_1	0.98	0.98	0.76	Fit
ρ_2	0.93	0.88	0.74	Fit
ω	0.300	0.325	0.370	Fit

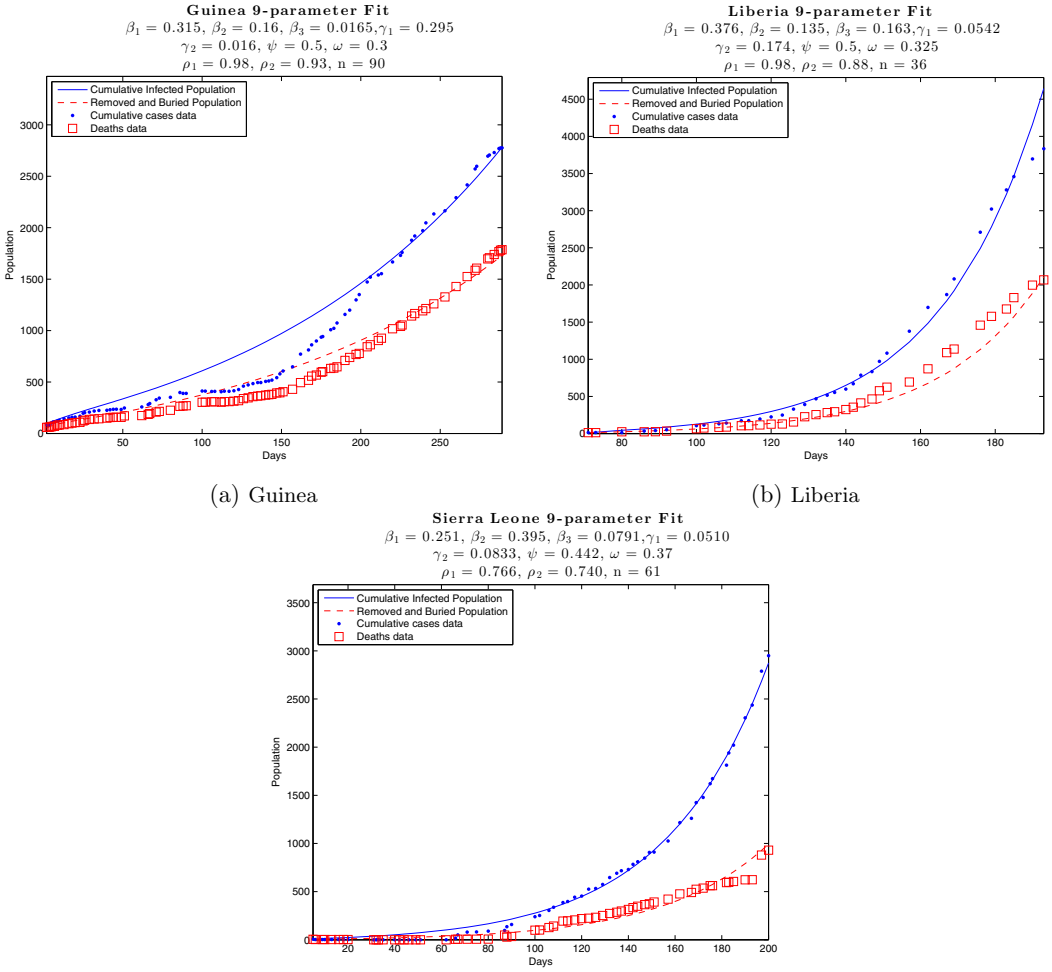

(a) Guinea (b) Liberia

(c) Sierra Leone

Fig. 2. Comparisons of fitted models to available date for Guinea, Liberia, and Sierra Leone.

With parameter values established, the basic reproduction number (i.e., the average number of secondary infections generated by a representative primary case within an entirely susceptible population) can be computed for each nation. Using the next generation matrix method (see Appendix), this quantity is found to be

$$R_0 = \frac{\beta_1 + \frac{\beta_2 \rho_1 \gamma_1}{\omega} + \frac{\beta_3}{\gamma_2}\psi}{\gamma_1 + \psi}. \tag{4}$$

Table 3
Basic reproduction numbers obtained from fit parameters.

Reproduction numbers			
Country	Guinea	Liberia	Sierra Leone
R_0	1.241	1.563	1.445

Table 4
Relevant parameter values in determining hospital placement. Here, the fatality rates from Ref. [19] have been used to compute these values, namely Liberia – 72.3% (unhospitalized), 67% (hospitalized) and Sierra Leone – 69% (unhospitalized) and 61.4% (hospitalized). Furthermore, these computed values are very similar to those determined by previous studies of Ebola epidemics [15,19].

Description	Liberia	Sierra Leone
Time to hospitalization	1.2 days	1.2 days
Time from hospitalization to death	4.38 days	10.09 days
Time from hospitalization to recovery	15.80 days	17.16 days
Time from symptom onset to death, unhospitalized	7.5 days	7.6 days
Time from symptom onset to recovery, unhospitalized	9.34 days	8.45 days
Time to proper burial	3.08 days	2.70 days
Proportion of hospitalized cases	0.57	0.60

Computation of R_0 can be broken into three distinct components that represent the respective contributions of the general community ($\frac{\beta_1}{\gamma_1+\psi}$), as well as transmissions arising from burial ($\frac{\beta_2\rho_1\gamma_1}{\omega(\gamma_1+\psi)}$) and hospitalization ($\frac{\beta_3\psi}{\gamma_2(\gamma_1+\psi)}$), and each of these terms can be further understood as the ratio of time to recovery to time to contact with respect to the aforementioned mode of transmission. We note that this quantity is independent of the parameters δ and ρ_2 since neither the length of the incubation period nor the death rate of hospitalized patients affects the generation of secondary infected cases. Additionally, the following result shows that the epidemic must decline rapidly whenever $R_0 < 1$, regardless of its initial state.

Theorem 1. *If $R_0 < 1$ the point $P = (1, 0, 0, 0, 0)$, which denotes the unique disease-free equilibrium of the proportion model (1), is globally asymptotically stable.*

As a consequence of this theorem, values of the basic reproduction number that are less than one imply that the E, I, H, and R_I compartments must tend to zero as $t \to \infty$. Hence, the total infected proportion of the population must vanish, thereby causing the disease to die out. As with many global stability theorems, the proof of this result relies on Lyapunov's direct method. For brevity, we postpone the proof until the Appendix.

Utilizing fitted parameter values the basic reproduction number for each nation was computed, as expressed within Table 3. Liberia appears to be experiencing the greatest detrimental effects of the epidemic, as evidenced by this metric, but the corresponding value for Sierra Leone is nearly as large, while Guinea does not differ too dramatically from the others. Without further intervention and new allocation of resources to fight the disease, our model predicts that the epidemic would continue to spread as of December 2014, generating a large number of new cases each day – 23 in Guinea, 119 in Sierra Leone, and 736 in Liberia. These figures predict an epidemic that is very close in size and scale to the true values compiled by the WHO and CDC [2,3].

3. Local metrics for resource allocation

Given the limited amount of resources available to these West African nations and the diminishing availability of external aid from charitable organizations around the world, a natural question to investigate is which of the nations currently experiencing an epidemic would benefit most from additional hospitalization and treatment resources. Thus, another major goal of this work is to study different metrics by which such decisions can be accurately established. Certainly, one way to answer this question is to compare the computed basic reproduction numbers for each region and allocate new resources to the one whose R_0 value is largest. However, this single value may not always capture a necessary level of detail within infection dynamics and doesn't account for parameter variation due to intervention. Hence, in this section we investigate both changes to R_0 and a few other possible metrics to determine the placement and allocation of new resources.

3.1. Fitted parameter values

Computing some of the specific mean times and probabilities (see Table 4) can provide a preliminary understanding of the epidemic. These quantities were derived directly from estimates of fatality rates provided by [19] and the parameter values (Table 2) fit to the data. For instance, the average time from patient hospitalization to death was computed using the parameters ρ_2 and γ_2. Namely, if t_{HD} represents this average time, and the fatality rate of all hospitalized cases in Liberia is 67%, as reported in [19], then the term $\rho_2\gamma_2$ within (1) can be represented as the product of the probability that

Table 5
Changes in $\Upsilon^{R_0}(\psi, \omega)$ at fitted values.

Sensitivities of reproduction number		
Country	Liberia	Sierra Leone
$\Upsilon^{R_0}_{\psi}(\psi_0, \omega_0)$	−0.3616	−0.3074
$\Upsilon^{R_0}_{\omega}(\psi_0, \omega_0)$	−0.0255	−0.0585

a hospitalized patient dies and the average rate at which a patient exits the hospitalized population due to death, or

$$\rho_2\gamma_2 = 0.67 \cdot \frac{1}{t_{HD}}.$$

Using the fitted values of ρ_2 and γ_2 in Liberia, one can uniquely determine t_{HD}. In the same way, the fit parameters ρ_1, γ_1, ψ, and ω were used to determine the remaining stated mean times for Liberia and Sierra Leone. These rates were not computed for Guinea as the behavior of the epidemic in this nation differs dramatically from the others, as noted in [15]. Because of this difference and the comparatively small value of R_0, we will disregard the spread of the disease within Guinea for the remainder of the paper.

Notice that Sierra Leone was determined to possess the longest average time from hospitalization to recovery and a larger percentage of hospitalized cases, while Liberia experiences the longer wait for proper burials on average. The two nations experience similar wait times for hospitalization. We further note that neither possesses uniformly larger infection rates, as transmission from the infected and hospitalized populations is largest in Liberia, but transmissions from deceased individuals is greatest in Sierra Leone. In addition, the number of infectious individuals and the rate of growth of the deceased population is largest within Liberia (Fig. 2). Other quantities, such as the proportion of the total population stricken with the disease, could also be considered. In general, parameter values alone, even when determined directly from the infected and deceased data sets, likely cannot determine the country most in need of additional resources.

3.2. Greatest reduction in R_0

Since an analysis of the basic reproduction number is a traditional metric to characterize the spread of disease, it is a natural quantity to consider reducing through intervention. In Section 2, values of R_0 were computed for each of the three nations. As a function of parameters within the model, the basic reproduction number is expressed by Eq. (4).

Until new pharmaceutical and enhanced medical treatments are developed, it appears that the parameters ρ_1, ρ_2, γ_1, and γ_2 cannot be greatly altered by the allocation of additional resources. Similar statements hold true for the infection parameters (β_1, β_1, β_3) and incubation period (δ), which are determined inherently by population interactions and the disease itself, though infection rates can be altered by changes in human behavior. The parameters over which one has the greatest immediate control and are most strongly altered by the addition of human resources are the hospitalization parameter ψ and rate of proper burial ω. Hence, we may fix the other parameters in the system and view R_0 as a function of ψ and ω. Then, the local rate of change of R_0 with respect to these parameters should provide insight into the efficacy of an increase in either resource. Using Eq. (4), we compute

$$\frac{\partial R_0}{\partial \psi} = \frac{-\beta_1 - \beta_2 \frac{\rho_1\gamma_1}{\omega} + \beta_3 \frac{\gamma_1}{\gamma_2}}{(\gamma_1 + \psi)^2}$$

and note that this quantity is negative if the numerator is negative. With parameter values from Table 2, the derivative is negative for each of the three nations, as one would expect a boost in the hospitalization rate ψ to lower the reproduction number. Similarly, we find

$$\frac{\partial R_0}{\partial \omega} = -\frac{\beta_2\rho_1\gamma_1}{(\gamma_1 + \psi)\omega^2},$$

and because all parameters are positive, this quantity must be negative as well. At this point, we may use these partial derivatives to gauge the local sensitivity of R_0, but a more descriptive quantity is the normalized forward sensitivity index [6], namely the ratio of the relative change in R_0 to the relative change in the parameter of interest, defined by

$$\Upsilon^{R_0}_p := \frac{\partial R_0}{\partial p} \cdot \frac{p}{R_0}$$

where $p \in \{\psi, \omega\}$. The quantities of interest for a nation are then the values of these normalized sensitivity indices, and we are particularly interested in how such values differ from their baselines, i.e. $\Upsilon^{R_0}_p$ evaluated at the current values of ψ or ω, which we denote by ψ_0 and ω_0 respectively. Computed values of these indices are displayed in Table 5. Additionally, contour plots of $R_0(\psi, \omega)$ for the two nations are displayed in Fig. 3. They clearly demonstrate that the influence of ψ is much greater than that of ω. Hence, an increase in the hospitalization of infected individuals would have a significantly greater impact on the reproduction number than devoting more resources to ensuring quick and proper burials of the deceased. Therefore, we reduce the problem to viewing R_0 as a function of ψ alone and investigate the relative impact that an increase

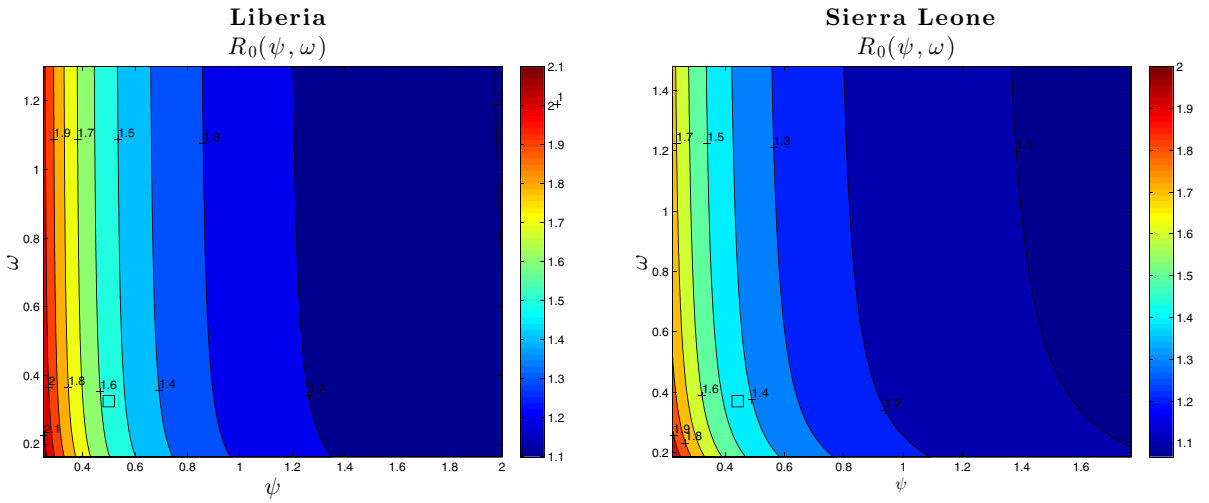

Fig. 3. Contour plots of $R_0(\psi, \omega)$. Parameters were varied from one-half their fitted value to four times this number. The black square represents the fit parameter pair (ψ_0, ω_0).

Table 6
Changes in $R_0(\psi)$ at differing ψ.

Marginal change in R_0		
Country	Liberia	Sierra Leone
$R_0'(\psi_0)$	−1.131	−1.005
$\inf_{\psi} R_0(\psi)$	0.937	0.948
$\sup_{\psi} R_0(\psi)$	7.344	5.740

in ψ may have on R_0. Hence, we fix $\omega = \omega_0$ and compute $R_0'(\psi_0)$ and for each country, the values of which are represented within Table 6. Of course, the values of $\Upsilon_{\psi}^{R_0}$ in Table 5 arise from those of $R_0'(\psi_0)$ in Table 6. Since $R_0'(\psi) < 0$ for all $\psi \geq 0$, the minimal value of R_0 is obtained by

$$\lim_{\psi \to \infty} R_0(\psi) = \frac{\beta_3}{\gamma_2}$$

while the maximal value occurs when no medical intervention is present and is

$$R_0(0) = \frac{\beta_1}{\gamma_1} + \frac{\beta_2 \rho_1}{\omega}.$$

These respective values are also provided within Table 6. The information described by $R_0(\psi)$ and $\Upsilon_{\psi}^{R_0}$ suggests that additional medical resources to boost the hospitalization parameter, and hence reduce the average time to hospitalization, will significantly impact both Liberia and Sierra Leone, with a slightly greater benefit to the former nation in comparison to the latter (as shown by Fig. 4).

3.3. Local sensitivity of the infected population

Another possible metric is the change in the infected population as a function of the hospitalization parameter ψ. As mentioned within the previous section, this parameter appears to be one of the most controllable factors of the disease's progression, and as we will show in the next section, it is the most influential in terms of the value of R_0. Hence, to conduct a local sensitivity analysis of the infected population as a function of ψ only, we fix all model parameters to their fitted value except for ψ. In particular, since this function $I(t; \psi)$ is also time-dependent we must rely on simulations of the system to approximate changes in this output over a period of time. This method was implemented with changes in ψ made at two differing points in time for Liberia and Sierra Leone. In both implementations the parameter ψ is varied between one half and twice its fitted value.

The first implementation focuses on changes in $I(t; \psi)$ arising from varying ψ at time $t = 0$, the beginning of the outbreak. Fig. 5 depicts the results of this analysis. In both countries, we see that increased values of ψ correspond to decreases in I. However, increasing ψ in Liberia produces a greater decrease in the infected population compared to that of Sierra Leone. This is evident due to the scales of the graphs in Fig. 5. The second implementation focuses on changes in

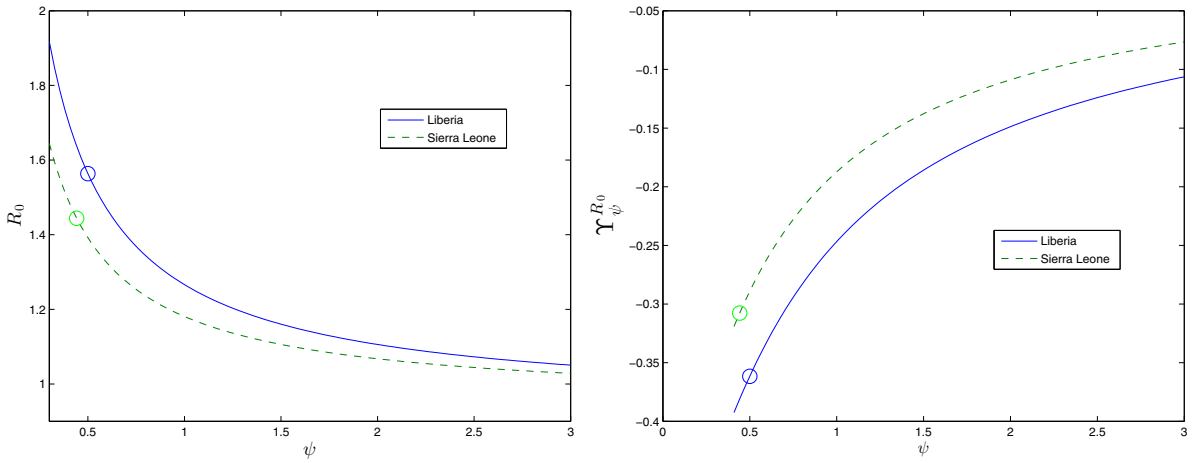

Fig. 4. Reproduction numbers by nation. R_0 as a function of hospitalization parameter (left) and the normalized forward sensitivity index of R_0 with respect to hospitalization parameter (right). The circles represent the values of these quantities at the hospitalization level obtained from data.

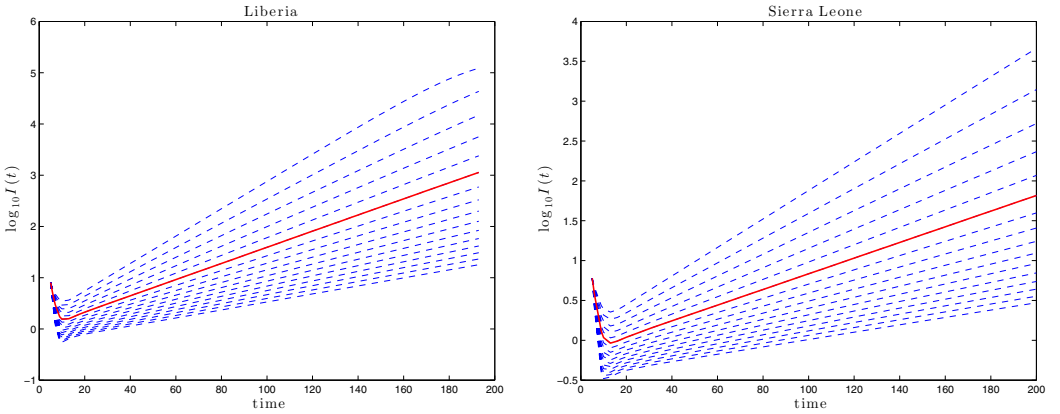

(a) Liberia (b) Sierra Leone

Fig. 5. Local sensitivity analysis of the infected population $I(t)$ (on a log-scale) as a function of the hospitalization parameter ψ. This parameter was varied from one-half its fitted value to twice this number. Notice the difference in scales between the nations.

$I(t;\ \psi)$ arising from altering the hospitalization parameter at the final recorded time of the data set, thereby simulating the implementation of new treatment strategies at the most recent time. The initial conditions used for future forecasting are given by the last day of the data set. For each value of ψ we forecast the model fifty days into the future. Fig. 6 summarizes the forecasting sensitivity analysis. Again, within both countries we see that increasing ψ reduces $I(t,\ \psi)$, but the reduction in Liberia is much greater than in Sierra Leone. In each of these cases, the local sensitivity of cumulative, rather than instantaneous, infections was also investigated and yielded similar results.

Hence, from this metric we conclude that variations in the hospitalization rate have a significant impact on the rate of infection within both Sierra Leone and Liberia. However, the largest impact is in the country of Liberia. A 30 percent increase in ψ leads to a nearly 1000 fewer infectious individuals in Liberia by the end of the forecasting simulation, while the same increase in Sierra Leone would result in a couple hundred fewer infectious individuals.

4. Global metrics for resource allocation

Though the local sensitivity analyses of the previous section were informative, none effectively captures the effects of large variations in model parameters on the quantity of interest. This occurs because evaluation of the partial derivatives of the reproduction number with respect to parameters must be performed at a specific point $\mathbf{x}$ in the input parameter space. Within the context of the Ebola model, input parameters can be represented by $\mathbf{x} = (\beta_1, \beta_2, \beta_3, \rho_1, \gamma_1, \gamma_2, \omega, \psi) \in \mathbb{R}^8$, while the input parameter space $\Omega \subset \mathbb{R}^8$ is defined by the ranges of each parameter in $\vec{x}$ as summarized in Table 7. Of course, the previous methods measured local sensitivity because model input parameters were perturbed about a specific point $\mathbf{x} \in \Omega$ in order to understand their effect on variations in the model output, e.g. $\frac{\partial R_0}{\partial \psi}(\vec{x})$. Contrastingly, *global* sensitivity metrics account for parameter variation across the entire input space Ω. Much like local measures of sensitivity, investigating

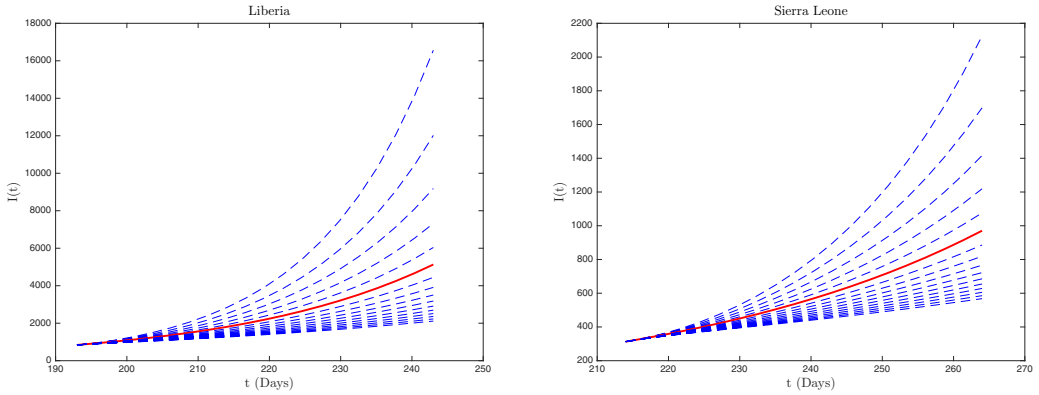

(a) Liberia (b) Sierra Leone

Fig. 6. Future sensitivity analysis of the infected population $I(t)$ with multiplicative variation of the hospitalization parameter ψ. This parameter was varied from $0.5\psi_0$ to $2\psi_0$ in $0.1\psi_0$ increments, with the solid line representing the fitted value. The lines above the solid line, at the final time, represent smaller values, while the lines below represent larger values of ψ.

Table 7
Intervals of parameter values for Liberia and Sierra Leone. Each of these parameters define the dimensions of the input parameter space Ω. Because this is a novel model, exact intervals for each parameter are neither known nor available. The intervals for the parameters β_1, β_2, β_3, and ω come from the constraints in the barrier method for fitting parameter values in Section 3.1. We used data from Ref. [19] to construct estimates of the remaining parameter intervals.

Parameter	Liberia	Sierra Leone
β_1	[0.1, 0.4]	[0.1, 0.4]
β_2	[0.1, 0.4]	[0.1, 0.4]
β_3	[0.05, 0.2]	[0.05, 0.2]
ρ_1	[0.41, 1]	[0.41, 1]
γ_1	[0.0276, 0.1702]	[0.0275, 0.1569]
γ_2	[0.081, 0.2100]	[0.1236, 0.3840]
ω	[0.25, 0.5]	[0.25, 0.5]
ψ	[0.0833, 0.7]	[0.0833, 0.7]

the global effects of input parameters can allow us to establish a relative notion of importance among the model inputs. One class of global sensitivity methods, known as *active subspace* methods, are particularly useful for models with a scalar quantity of interest [7,8]. As the scalar reproduction number R_0 is a particular quantity of interest in epidemiological models and this metric is a strong indicator of the behavior of the disease, we will utilize active subspaces to perform a global sensitivity analysis of $R_0(\vec{x})$.

To simplify our calculations we first shift and scale the parameter space of dimension eight to the hypercube $\Omega' = [-1, 1]^8$ and equip it with a uniform probability density, $\rho(\vec{x}) = 2^{-8}$. The choice of a uniform density limits our assumptions and details the lack of *a priori* knowledge of the most likely parameter values, as we are assigning equal likelihood to all values within the given range. Of course, as additional statistical research is conducted concerning parameters in the model (e.g., transmission, fatality, and recovery rates), a more comprehensive understanding of the distributions of these parameters will be obtained, and $\rho(\vec{x})$ can be easily altered to better describe our current knowledge of disease dynamics.

Given the normalized parameter space and the associated density, active subspaces of the parameter space are defined in terms of the eigenpairs of the 8×8 positive, semi-definite matrix

$$\boldsymbol{C} := \int_{\Omega'} \nabla R_0(\vec{x}) \nabla R_0^T(\vec{x}) \rho(\vec{x}) d\vec{x} = \boldsymbol{W} \Lambda \boldsymbol{W}^T, \tag{5}$$

where $\boldsymbol{W} = [\vec{w}_1, \ldots, \vec{w}_8]$ is the orthogonal matrix of normalized eigenvectors of $\boldsymbol{C}$, $\Lambda = \mathrm{diag}(\lambda_1, \ldots, \lambda_8)$ is the corresponding diagonal matrix of eigenvalues arranged in decreasing order, and $\nabla R_0(\vec{x})$ is the gradient expressed as a column vector. In particular, the eigenpairs satisfy the relationship

$$\lambda_i = \int (\nabla R_0^T \vec{w}_i)^2 \, \rho \, d\vec{x}. \tag{6}$$

Notice that if $\lambda_i = 0$ for some $i \in \{1, \ldots, 8\}$, then R_0 is constant along the direction $\vec{w}_i$, and therefore no change in this model output occurs from variations along the $\vec{w}_i$ direction of the parameter input space. Such structure can be exploited to reduce the dimension of the model. For instance, suppose $\lambda_{n+1} \ll \lambda_n$ for some $n < 7$. Then, we partition the orthogonal

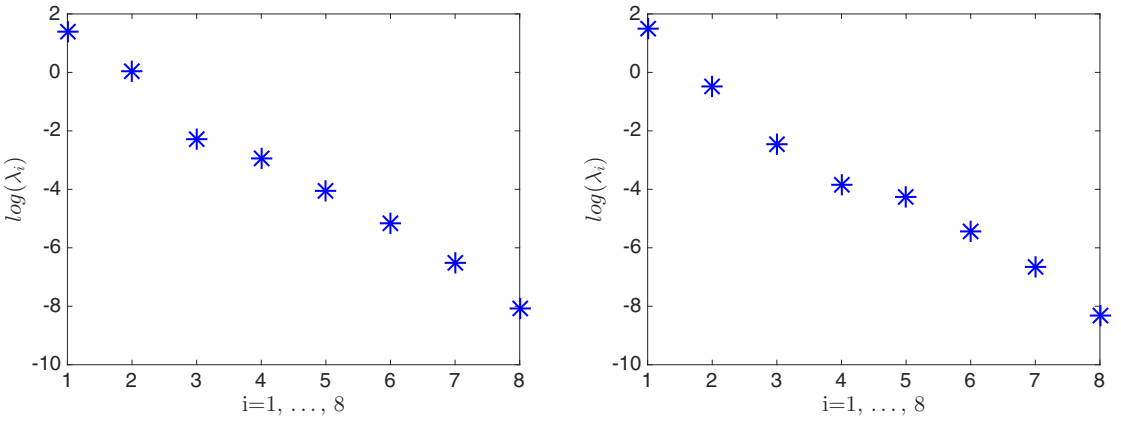

Fig. 7. Magnitudes of the eigenvalues $\mathbf{\Lambda}$ from Eq. (5) on a logscale. The gap between the second and third eigenvalues for both Liberia and Sierra Leone suggests a two-dimensional active subspace, i.e., $n = 2$. The computation of the matrix $\boldsymbol{C} = \boldsymbol{W}\boldsymbol{\Lambda}\boldsymbol{W}^T$ in (5) (and therefore the eigenvalues) is done via tensor product Gauss–Legendre quadrature on 8^8 points (eight per parameter dimension).

decomposition of $\boldsymbol{C}$ into

$$\Lambda = \begin{bmatrix} \Lambda_1 & \\ & \Lambda_2 \end{bmatrix}, \qquad \boldsymbol{W} = \begin{bmatrix} \boldsymbol{W}_1 & \boldsymbol{W}_2 \end{bmatrix}, \tag{7}$$

where Λ_1 is a diagonal matrix of the first n eigenvalues, and $\boldsymbol{W}_1$ is the $8 \times n$ matrix containing the first n eigenvectors. To identify an active subspace for the basic reproductive number (i.e. a linear subspace of the parameter space defined by the span of the directions of strongest variability in R_0), we must estimate the eigenpairs Λ, $\boldsymbol{W}$ and identify a gap amongst the eigenvalues. Because the dimension of our parameter space is relatively small we use high order numerical integration rules to estimate $\boldsymbol{C}$ in (5). More specifically, we use tensor product Gauss–Legendre quadrature on 8^8 points (eight per parameter dimension).

Next, define $\alpha \in \mathbb{R}^8$ by

$$\alpha \; = \; \alpha(n) \; = \; \sum_{j=1}^{n} \lambda_j \vec{w}_j^2, \tag{8}$$

where the exponent on the vector $\vec{w}_j$ denotes an elementwise exponentiation, i.e. within each component of $\vec{w}_j$. The entries of the vector $\alpha(n)$ are referred to as the *activity scores* of $\boldsymbol{C}$, and we use these numbers to rank the importance of the input parameters for the quantity of interest R_0. The active subspace's construction provides insight into the interpretation of the activity scores [7, Chapter 3]. Namely, the eigenvector $\vec{w}_1$ identifies the most important direction in the parameter space in the following sense: perturbing $\vec{x}$ along $\vec{w}_1$ changes R_0 more, on average, than perturbing $\vec{x}$ orthogonal to $\vec{w}_1$, as demonstrated in (6). The components of $\vec{w}_1$ measure the relative change in each component of $\vec{x}$ along this most important direction, so they impart significance to each component of $\vec{x}$. The second most important direction is the eigenvector $\vec{w}_2$, and the relative importance of $\vec{w}_2$ is measured by the difference between the eigenvalues λ_1 and λ_2. For example, if $\lambda_1 \gg \lambda_2$, then $R_0(\vec{x})$ possesses a dominant one-dimensional active subspace, and the importance of the components of $\vec{x}$ is captured by the components of $\vec{w}_1$. Therefore, to construct this global sensitivity metric, it is reasonable to scale each eigenvector by its corresponding eigenvalue.

The results of computing the eigenvalues λ_i $(i = 1, \ldots, 8)$ and pertinent eigenvector $\vec{w}_1$ for $\boldsymbol{C}$ are presented in Figs. 7 and 8, respectively. Notice that eigenvalues are displayed on a log scale, and thus a notable (nearly two orders of magnitude) spectral gap occurs between λ_1 and λ_2 for each nation. Hence, $\vec{w}_1$ displays the parameters of greatest global importance to R_0, and we see that it is ψ which is responsible for the greatest decrease in this output variable within either country. This further justifies the omission of variations in other parameters within the local analysis of previous sections since, on average, they influence R_0 much less than ψ. As an additional benefit of the active subspace method, we note that the computed activity score is actually independent of the values of parameters estimated from the data, e.g. ω_0 and ψ_0. Instead, we merely require a suitable range of parameter values in order to implement the method, and this can be much easier to obtain than a realistic fit of parameters from case data which tracks infected and deceased individuals. As noted within Table 7 the intervals for these parameter values are easily obtained as rate coefficients from compiled statistics [19], such as the mean time from infection to recovery or infection to death.

Revisiting Fig. 7, a logical argument can be made that an even larger spectral gap occurs within λ_2 and λ_3 for each nation. Thus, we have computed the corresponding activity scores $\alpha(2)$ for each country and the resulting vector is shown in Fig. 9. Here, we see that the activity score for ψ within both $\alpha(1)$ and $\alpha(2)$ is significantly greater within Sierra Leone

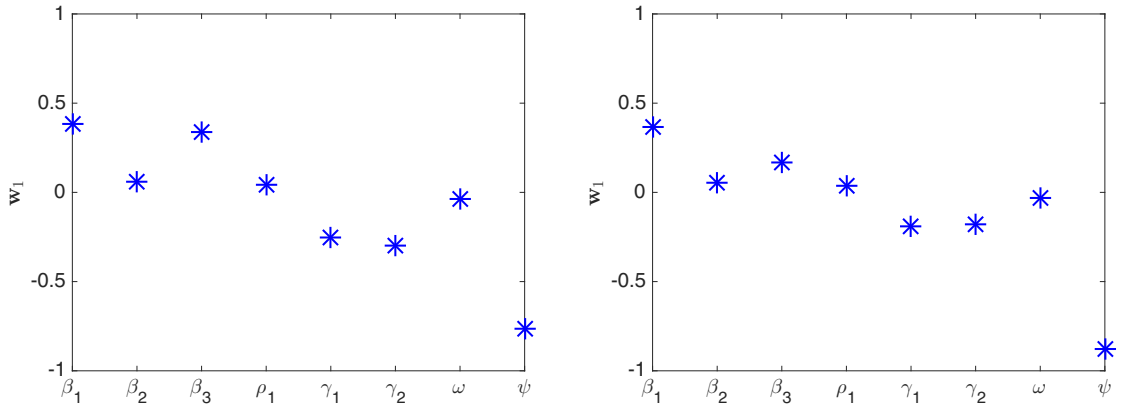

(a) Liberia (b) Sierra Leone

Fig. 8. Components of the first eigenvector of $\boldsymbol{W}_1$ in (7). Each component corresponds to a different parameter as indicated. The sign of the components inform us as to how, on average, changes in the parameter correspond to changes in R_0. We see that the parameter corresponding to the greatest decrease in R_0, in both countries is ψ. The computation of the matrix $\boldsymbol{C} = \boldsymbol{W}\boldsymbol{\Lambda}\boldsymbol{W}^T$ in (5) (and therefore the eigenvectors) is done via tensor product Gauss–Legendre quadrature on 8^8 points (eight per parameter dimension).

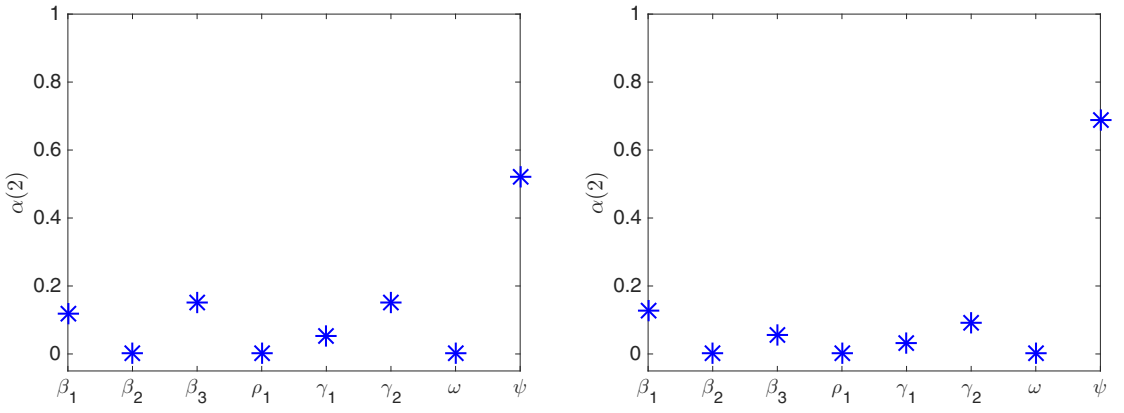

(a) Liberia (b) Sierra Leone

Fig. 9. Activity scores, normalized to 1. This was computed using $n = 2$, the dimension of the active subspace. In both countries, the parameter ψ is by far the most influential on the reproductive ratio. We may also conclude that the parameters β_2, ρ_1, and ω have negligible influence on R_0 in both Liberia and Sierra Leone. The computation of the matrix $\boldsymbol{C} = \boldsymbol{W}\boldsymbol{\Lambda}\boldsymbol{W}^T$ in (5) (and therefore the activity scores) is done via tensor product Gauss–Legendre quadrature on 8^8 points (eight per parameter dimension).

than in Liberia. This result suggests that if resources can be allocated so that the hospitalization rate within either country is altered enough to render its current (or fitted) value insignificant, then the basic reproduction number would experience a greater decrease by increasing the hospitalization rate in Sierra Leone rather than Liberia. Thus, the benefit of the active subspace method becomes clear – if large variations of model input parameters are realistic, then the global sensitivity metric provided by this method serves as a better decision-making tool than a classical, derivative-based local sensitivity approach. In particular, a local analysis suggests that allocating more resources for hospitalization within Liberia would have a larger impact than doing so within Sierra Leone, while a global analysis suggests the opposite.

5. Conclusions and future work

To gain insight into the spread of the most recent Ebola epidemic within Western Africa, a modified SEIR model was constructed that incorporates the effects of interaction amongst infectious individuals, including those who have succumb to the disease, and the population of susceptible individuals. Upon creating the model, parameter values were fit to known WHO case data [22] gathered between March and December 2014 for Guinea, Liberia, and Sierra Leone. Local metrics were then proposed to determine the optimal allocation of additional medical resources, and the local analysis clearly established that Liberia would most benefit, via a reduced R_0, from an increase in the hospitalization rate. Finally, a novel global sensitivity metric was proposed and explored to allow for a greater understanding of model output responses to changes

within input parameters, which suggested that Sierra Leone, and not Liberia, would benefit most. All of the software used to develop these tools has been compiled at

https://github.com/PaulMDiaz/Ebola

and is freely available to any parties wishing to further the results of the article.

Given the results of the previous sections, one must conclude that the optimal placement for treatment facilities in Western Africa depends largely on the amount of new resources that can be devoted to a specific country. If resources are scarce and parameters cannot deviate significantly from their current values, then local metrics imply that Liberia will experience the greatest benefit from additional resources. This can be seen in many ways, as Liberia possesses the larger current value of R_0, the smaller proportion of hospitalized cases, the greater rate of decrease in $R_0(\psi)$, and the greatest decrease in the infected population as ψ is varied. Contrastingly, if the introduction of new resources can drastically alter parameters within the model, then the global activity scores are the pertinent metric, and they indicate that Sierra Leone will derive the greater benefit. In either case, our methods have clearly demonstrated the importance of the hospitalization rate amongst all other parameters which appear in the model. Namely, Figs. 8 and 9 show that the parameter ψ has the largest impact on reducing R_0 in both Liberia and Sierra Leone. Furthermore, Fig. 9 confirms our initial finding that the parameter ω, as well as β_2 and γ_1, has very little influence on the basic reproduction number R_0.

The conclusions drawn herein are further supported by the conclusion of the Ebola epidemic in Liberia in 2015. In December of 2014, The People's Republic of China placed new treatment facilities within Liberia [12]; subsequently, there was a vast improvement in controlling the spread of the infection, and Liberia was declared Ebola-free on January 14, 2016. Given a current and detailed data set, the tools developed within the current study, including the modified SEIR model, the process for parameter estimation, and both local and global metrics for determining the need for hospital resources, could all be used to identify optimal resource allocation strategies for future epidemics.

Acknowledgments

The authors would like to thank Sara Del Valle in the Energy and Infrastructure Analysis group at Los Alamos National Laboratory for working with the PIC Math program, suggesting the problem of interest, and providing helpful discussions and advice.

Appendix. Steady states, basic reproduction number, and stability

To determine any non-zero steady state solutions, the rates of change for the S, E, I, H, and R_I populations were set to zero. As previously described, the equations for the removed-buried and removed-recovered populations decouple from the model and thus were omitted. With this, we find

$$\left.\begin{aligned} \frac{dS}{dt} &= -S(\beta_1 I + \beta_2 R_I + \beta_3 H) = 0 \\ \frac{dE}{dt} &= \beta_1 SI + \beta_2 SR_I + \beta_3 SH - \delta E = 0 \end{aligned}\right\} \tag{A.1}$$

and

$$\left.\begin{aligned} \frac{dI}{dt} &= \delta E - \gamma_1 I - \psi I = 0 \\ \frac{dH}{dt} &= \psi I - \gamma_2 H = 0 \\ \frac{dR_I}{dt} &= \rho_1 \gamma_1 I - \omega R_I = 0. \end{aligned}\right\} \tag{A.2}$$

The three equations within (A.2) then imply

$$E = \frac{\gamma_1 + \psi}{\delta} I, \qquad H = \frac{\psi}{\gamma_2} I, \qquad R_I = \frac{\rho_1 \gamma_1}{\omega} I,$$

so that substitution of these expressions into (A.1) yields

$$\left.\begin{aligned} SI\left(\beta_1 + \frac{\beta_2 \rho_1 \gamma}{\omega} + \frac{\beta_3 \psi}{\gamma_2}\right) &= 0 \\ I\left[-(\gamma_1 + \psi) + S\left(\beta_1 + \frac{\beta_2 \rho_1 \gamma_1}{\omega} + \frac{\beta_3 \psi}{\gamma_2}\right)\right] &= 0. \end{aligned}\right\} \tag{A.3}$$

Notice that within (A.3), $S = 0$ is one possible solution, which implies $I = 0$ and that all populations are zero. As we assume throughout that the total population satisfies $N > 0$, this steady state is not possible. Instead, imposing $I = 0$ within (A.3), we see that S is arbitrary. However, to satisfy the total population constraint, we must have $S = 1$. Hence, we find the unique disease-free equilibrium $(\bar{S}, \bar{E}, \bar{I}, \bar{H}, \bar{R}_I) = (1, 0, 0, 0, 0)$.

To compute the basic reproduction number of the system with respect to this equilibrium, we employ the Next Generation Matrix method [17]. In particular, computing the gains and losses matrices associated with (1), we find

$$F = \begin{pmatrix} 0 & \beta_1\bar{S} & \beta_3\bar{S} & \beta_2\bar{S} \\ 0 & 0 & 0 & 0 \\ 0 & 0 & 0 & 0 \\ 0 & 0 & 0 & 0 \end{pmatrix}$$

and

$$V = \begin{pmatrix} \delta & 0 & 0 & 0 \\ -\delta & \gamma_1+\psi & 0 & 0 \\ 0 & -\psi & \gamma_2 & 0 \\ 0 & -\rho_1\gamma_1 & 0 & \omega \end{pmatrix}.$$

Here, F has been evaluated at the equilibrium determined above. Inverting V yields

$$V^{-1} = \begin{pmatrix} \frac{1}{\delta} & 0 & 0 & 0 \\ \frac{1}{\gamma_1+\psi} & \frac{1}{\gamma_1+\psi} & 0 & 0 \\ \frac{\psi}{\gamma_2(\gamma_1+\psi)} & \frac{\psi}{\gamma_2(\gamma_1+\psi)} & \frac{1}{\gamma_2} & 0 \\ \frac{\rho_1\gamma_1}{\omega(\gamma_1+\psi)} & \frac{\rho_1\gamma_1}{\omega(\gamma_1+\psi)} & 0 & \frac{1}{\omega} \end{pmatrix}$$

and, using $\bar{S} = 1$, the resulting next generation matrix is

$$FV^{-1} = \begin{pmatrix} \frac{\beta_1 + \frac{\beta_2\rho_1\gamma_1}{\omega} + \frac{\beta_3}{\gamma_2}\psi}{\gamma_1+\psi} & \frac{\beta_1 + \frac{\beta_2\rho_1\gamma_1}{\omega} + \frac{\beta_3}{\gamma_2}\psi}{\gamma_1+\psi} & \beta_3\gamma_2 & \beta_2\omega \\ 0 & 0 & 0 & 0 \\ 0 & 0 & 0 & 0 \\ 0 & 0 & 0 & 0 \end{pmatrix}.$$

It is easy to see that the spectral radius of this matrix is exactly $\left(FV^{-1}\right)_{1,1}$ as the remaining eigenvalues must be identically zero. Thus, we arrive at an explicit formula for the basic reproduction number, namely

$$R_0 := \rho\left(FV^{-1}\right) = \frac{\beta_1 + \frac{\beta_2\rho_1\gamma_1}{\omega} + \frac{\beta_3}{\gamma_2}\psi}{\gamma_1+\psi}.$$

Finally, we complete the Appendix with the proof of Theorem 1.

Proof. We first note that the assumption $R_0 < 1$ directly implies the condition

$$\beta_1 + \beta_2\frac{\rho_1\gamma_1}{\omega} + \beta_3\frac{\psi}{\gamma_2} - (\gamma_1+\psi) < 0. \tag{A.4}$$

Next, define

$$\Gamma := \{(S,E,I,H,R_I) \in \mathbb{R}^5_+ : 0 \le S+E+I+H+R_I \le 1\}$$

and note that this is an invariant set under the flow generated by Eq. (1). Further denote the point $P = (1,0,0,0,0) \in \Gamma$ and define the function $\mathcal{V} \in C^1(\Gamma)$ by

$$\mathcal{V}(S,E,I,H,R_I) = S - 1 - \ln(S) + E + I + \frac{\beta_3}{\gamma_2}H + \frac{\beta_2}{\omega}R_I.$$

Notice that

$$\mathcal{V}(1,0,0,0,0) = 0,$$

and since $S > 1 + \ln(S)$ for all $S \in (0,1)$, it follows that

$$\mathcal{V}(x) > 0 \quad \text{for all} x \in \Gamma \setminus \{P\}.$$

Finally, we compute the time derivative of $\mathcal{V}$ along trajectories in (1) and use (A.4) to find

$$\begin{aligned} \dot{\mathcal{V}}(S,E,I,H,R_I) &= (S-1)\frac{1}{S}\frac{dS}{dt} + \frac{dE}{dt} + \frac{dI}{dt} + \frac{\beta_3}{\gamma_2}\frac{dH}{dt} + \frac{\beta_2}{\omega}\frac{dR_I}{dt} \\ &= (1-S)(\beta_1 I + \beta_2 R_I + \beta_3 H) + S(\beta_1 I + \beta_2 R_I + \beta_3 H) \end{aligned}$$

$$
\begin{aligned}
&-(\gamma_1+\psi)I+\frac{\beta_3}{\gamma_2}(\psi I-\gamma_2 H)+\frac{\beta_2}{\omega}(\rho_1\gamma_1 I-\omega R_I)\\
&=\left[\beta_1+\beta_2\frac{\rho_1\gamma_1}{\omega}+\beta_3\frac{\psi}{\gamma_2}-(\gamma_1+\psi)\right]I\\
&\leq 0
\end{aligned}
$$

for $(S, E, I, H, R_I)\in\Gamma$. Because $\dot{\mathcal{V}}=0$ if and only if $I=0$, we see that P is the maximal invariant set in $\{x\in\Gamma:\dot{\mathcal{V}}(x)=0\}$. Therefore, the global asymptotic stability of P follows from LaSalle's invariance principle, and the proof is complete. □

References

[1] J. Astacio, D. Briere, M. Guillen, J. Martınez, F. Rodrıguez, and N. Valenzuela-Campos, Mathematical models to study the outbreaks of Ebola, Tech. Report Biometrics Unit Technical report BU-1365-M, retrieved from https://ecommons.library.cornell.edu/bitstream/1813/31962/1/BU-1365-M.pdf, Cornell University, 1996.

[2] Centers for Disease Control and Prevention, 2014 Ebola outbreak in West Africa – case counts, 2014, (Accessed: 02/10/2017). https://www.cdc.gov/vhf/ebola/outbreaks/2014-west-africa/case-counts.html.

[3] Centers for Disease Control and Prevention, Ebola virus disease outbreak – West Africa, 2014, (Accessed: 02/10/2017). https://www.cdc.gov/mmwr/preview/mmwrhtml/mm6325a4.htm.

[4] Centers for Disease Control and Prevention, Questions and answers: estimating the future number of cases in the Ebola epidemic – Liberia and Sierra Leone, 2014–2015, 2014, (Accessed: 01/10/2016). http://www.cdc.gov/vhf/ebola/outbreaks/2014-west-africa/qa-mmwr-estimating-future-cases.html.

[5] Centers for Disease Control and Prevention, Ebola virus disease, 2015, http://www.cdc.gov/vhf/ebola/treatment/index.html. (Accessed: 12/28/2015).

[6] N. Chitnis, J. Hyman, J. Cusching, Determining important parameters in the spread of malaria through the sensitivity analysis of a mathematical model, Bull. Math. Bio. 70 (5) (2008) 1272–1296.

[7] P.G. Constantine, Active Subspaces: Emerging Ideas for Dimension Reduction in Parameter Studies, SIAM, 2015.

[8] P.G. Constantine, P. Diaz, Global sensitivity metrics from active subspaces, Reliability Engineering & System Safety 162 (2017) 1–13.

[9] M.G. Dixon, I.J. Schafer, et al., Ebola viral disease outbreak in West Africa, MMWR Morb. Mortal Wkly. Rep. 63 (25) (2014) 548–551.

[10] A. Du Toit, Ebola virus in West Africa, Nat. Rev. Microbiol. 12 (2014) 312.

[11] J. Legrand, R.F. Grais, P.-Y. Boelle, A.-J. Valleron, A. Flahault, Understanding the dynamics of Ebola epidemics, Epidemiol. Infect. 135 (04) (2007) 610–621.

[12] Médecins Sans Frontières (MSF) International, Ebola response: where are we now?, 2014, (Accessed: 12/28/2015). https://www.doctorswithoutborders.org/sites/usa/files/ebola_briefing_paper_12.14.pdf.

[13] A. Pandey, K.E. Atkins, J. Medlock, N. Wenzel, J.P. Townsend, J.E. Childs, T.G. Nyenswah, M.L. Ndeffo-Mbah, A.P. Galvani, Strategies for containing Ebola in West Africa, Science 346 (6212) (2014) 991–995.

[14] C. Rivers, Virgina Tech network dynamics and simulation science laboratory, 2015, (Accessed: 01/09/2016). https://github.com/cmrivers/ebola/blob/master/country_timeseries.csv.

[15] C.M. Rivers, E.T. Lofgren, M. Marathe, S. Eubank, B.L. Lewis, Modeling the impact of interventions on an epidemic of Ebola in Sierra Leone and Liberia, PLoS Currents Outbreaks. 2014 Oct 16. Edition 1. doi:10.1371/currents.outbreaks.fd38dd85078565450b0be3fcd78f5ccf.

[16] J. Shaman, W. Yang, S. Kandula, Inference and forecast of the current West African Ebola outbreak in Guinea, Sierra Leone and Liberia, PLoS Curr. 6 (2014).

[17] P. Van den Driessche, J. Watmough, Reproduction numbers and sub-threshold endemic equilibria for compartmental models of disease transmission, Math. Biosci. 180 (1) (2002) 29–48.

[18] G. Webb, C. Browne, X. Huo, O. Seydi, M. Seydi, P. Magal, A model of the 2014 Ebola epidemic in West Africa with contact tracing, PLoS Curr. 7 (2014).

[19] WHO Ebola Response Team, Ebola virus disease in West Africa – The first 9 months of the epidemic and forward projections, New Engl. J. Med. 371 (16) (2014) 1481–1495, doi:10.1056/NEJMoa1411100. PMID: 25244186

[20] World Health Organization, Field situation: how to conduct safe and dignified burial of a patient who has died from suspected or confirmed Ebola virus disease, 2014. (Accessed: 01/09/2016). http://www.who.int/csr/resources/publications/ebola/safe-burial-protocol/en/).

[21] World Health Organization, New WHO safe and dignified burial protocol – Key to reducing Ebola transmission, 2014b, (Accessed: 01/09/2016). http://www.who.int/mediacentre/news/notes/2014/ebola-burial-protocol/en/).

[22] World Health Organization, Ebola situation report – 29 April 2015, 2015, (Accessed: 01/09/2016). http://apps.who.int/ebola/current-situation/ebola-situation-report-29-april-2015.

[23] World Health Organization, Frequently asked questions on Ebola virus disease, 2016, (Accessed: 01/09/2016). http://www.who.int/csr/disease/ebola/faq-ebola/en/.